

Published in final edited form as:

*J Mol Cell Cardiol.* 2012 November ; 53(5): 707–714. doi:10.1016/j.yjmcc.2012.08.012.

## 5-HT<sub>2B</sub> antagonism arrests non-canonical TGF- $\beta$ 1-induced valvular myofibroblast differentiation

Joshua D. Hutcheson<sup>1</sup>, Larisa M. Ryzhova<sup>1</sup>, Vincent Setola<sup>2</sup>, and W. David Merryman<sup>1,\*</sup>

<sup>1</sup>Department of Biomedical Engineering, Vanderbilt University, Nashville, TN

<sup>2</sup>Department of Pharmacology, University of North Carolina, Chapel Hill, NC

### Abstract

Transforming growth factor- $\beta$ 1 (TGF- $\beta$ 1) induces myofibroblast activation of quiescent aortic valve interstitial cells (AVICs), a differentiation process implicated in calcific aortic valve disease (CAVD). The ubiquity of TGF- $\beta$ 1 signaling makes it difficult to target in a tissue specific manner; however, the serotonin 2B receptor (5-HT<sub>2B</sub>) is highly localized to cardiopulmonary tissues and agonism of this receptor displays pro-fibrotic effects in a TGF- $\beta$ 1-dependent manner. Therefore, we hypothesized that antagonism of 5-HT<sub>2B</sub> opposes TGF- $\beta$ 1-induced pathologic differentiation of AVICs and may offer a druggable target to prevent CAVD. To test this hypothesis, we assessed the interaction of 5-HT<sub>2B</sub> antagonism with canonical and non-canonical TGF- $\beta$ 1 pathways to inhibit TGF- $\beta$ 1-induced activation of isolated porcine AVICs *in vitro*. Here we show that AVIC activation and subsequent calcific nodule formation is completely mitigated by 5-HT<sub>2B</sub> antagonism. Interestingly, 5-HT<sub>2B</sub> antagonism does not inhibit canonical TGF- $\beta$ 1 signaling as identified by Smad3 phosphorylation and activation of a partial plasminogen activator inhibitor-1 promoter (PAI-1, a transcriptional target of Smad3), but prevents non-canonical p38 MAPK phosphorylation. It was initially suspected that 5-HT<sub>2B</sub> antagonism prevents Src tyrosine kinase phosphorylation; however, we found that this is not the case and time-lapse microscopy indicates that 5-HT<sub>2B</sub> antagonism prevents non-canonical TGF- $\beta$ 1 signaling by physically arresting Src tyrosine kinase. This study demonstrates the necessity of non-canonical TGF- $\beta$ 1 signaling in leading to pathologic AVIC differentiation. Moreover, we believe that the results of this study suggest 5-HT<sub>2B</sub> antagonism as a novel therapeutic approach for CAVD that merits further investigation.

### Keywords

heart valves; calcification; TGF- $\beta$ 1; serotonin receptors

### Introduction

The lack of a therapeutic treatment for calcific aortic valve disease (CAVD) limits the clinical options available to patients, and this often results in physicians opting to delay

© 2012 Elsevier Ltd. All rights reserved.

\* To whom correspondence should be addressed: Department of Biomedical Engineering, Vanderbilt University, 2213 Garland Ave., 9445 MRB IV, Nashville, TN 37232-0493, P: 615.322.7219, F: 615.343.6541, david.merryman@vanderbilt.edu.

**Publisher's Disclaimer:** This is a PDF file of an unedited manuscript that has been accepted for publication. As a service to our customers we are providing this early version of the manuscript. The manuscript will undergo copyediting, typesetting, and review of the resulting proof before it is published in its final citable form. Please note that during the production process errors may be discovered which could affect the content, and all legal disclaimers that apply to the journal pertain.

**Disclosures:** none declared

surgical intervention until aortic valve (AV) replacement is absolutely necessary, leading to diminished AV function in the meantime. The development of a suitable therapeutic for CAVD depends on the ability to target the root etiology of the disease, which at the cellular level, is believed to be caused by activation of AV interstitial cells (AVICs) from a quiescent fibroblastic phenotype to a contractile myofibroblast phenotype characterized by the expression of smooth muscle  $\alpha$ -actin ( $\alpha$ SMA) and SM22 $\alpha$  [1–2]. Once activated, AVICs increase extracellular matrix deposition, leading to the fibrotic changes characteristic of the onset of CAVD [3]. End-stage CAVD is characterized by the formation of bone-like calcific nodules within stenotic leaflets, severely compromising the biomechanical integrity of the AV [4]. In order to develop a strategy to prevent CAVD, a more thorough understanding of the cellular signaling that leads to the subsequent tissue level changes involved in the progression of CAVD is needed to elucidate relevant therapeutic targets.

Transforming growth factor- $\beta$ 1 (TGF- $\beta$ 1) is highly expressed in diseased AV leaflets and has been the most extensively studied cytokine initiator of AVIC activation and CAVD [1, 4–5]. TGF- $\beta$ 1 ligand binding at its type II receptor (T $\beta$ RII) leads to recruitment and activation of the type I T $\beta$ R, Alk5, which canonically elicits a wide variety of cellular processes by signaling through the transcription factors Smads 2 and 3 [6]. Many studies have also focused on non-canonical signaling pathways to explain the myriad of cellular responses induced by TGF- $\beta$ 1 ligand binding, and p38 MAPK pathways have been identified as key mediators of cellular processes such as cell migration and mesenchymal transformations [7–9], which are characterized by upregulation of contractile elements similar to those identified in myofibroblast activation. In addition, recent studies have demonstrated that TGF- $\beta$ 1-induced phosphorylation of p38 in epithelial cells is dependent upon phosphorylation of T $\beta$ RII by Src tyrosine kinase [10].

Unfortunately, the ubiquity associated with its signaling makes direct inhibition of TGF- $\beta$ 1 a poor therapeutic strategy for CAVD. Further, the relative contributions of canonical and non-canonical TGF- $\beta$ 1 signaling in leading to myofibroblast activation of AVICs are unknown. Here, we were interested in studying the interaction between a specific G protein-coupled receptor (GPCR) highly localized to cardiopulmonary tissues, the serotonin 2B receptor (5-HT<sub>2B</sub>), with TGF- $\beta$ 1 signaling, and assessing the potential of targeting this receptor for prevention of CAVD. The motivation for this study stems from the finding that agonism of 5-HT<sub>2B</sub> was the major culprit in the development of pathologic AV alterations that led to the recall of norfenfluramine, a popular drug used to treat obesity, and pergolide, a drug used to treat Parkinson's disease [11–12]. 5-HT<sub>2B</sub> agonists were found to lead to AVIC myofibroblast activation in a TGF- $\beta$ 1-dependent manner [13–14]; therefore, we hypothesized that antagonism of 5-HT<sub>2B</sub> opposes TGF- $\beta$ 1-mediated myofibroblast activation of AVICs. In support of our hypothesis, antagonism of 5-HT<sub>2B</sub> has been shown to induce anti-fibrotic responses in animal models of cardiac hypertrophy and pulmonary fibrosis [15–16]; however, the molecular mechanisms of this action remain unclear, and the ability of 5-HT<sub>2B</sub> antagonism to directly inhibit TGF- $\beta$ 1-mediated myofibroblast activation of AVICs has not been examined. We believe that the results of this study may lead to novel therapeutic strategies for CAVD and should be studied further.

## Methods

### AVIC Isolation and Culture

AVICs were isolated from porcine valves obtained from a local abattoir by dissecting the valve cusps from the surrounding muscle and digested with collagenase. Isolated AVICs were then cultured at 37°C and 5% CO<sub>2</sub> on T-75 tissue culture treated flasks in cell growth media consisting of DMEM supplemented with 10% fetal bovine serum (FBS), 1% penicillin/streptomycin antibiotic, and 1% amphotericin B antifungal. Previous studies have

shown that AVICs retain phenotypic plasticity up to 10 passages after initial harvest [17]. We have observed phenotypic changes as early as 7 passages after harvest; therefore, we did not exceed this maximum limit and for this study, when AVICs ceased to respond to TGF- $\beta$ 1 treatment, as indicated by  $\alpha$ SMA expression, they were excluded.

### Antagonist and Inhibitor Treatments

For all assays of AVIC activation ( $\alpha$ SMA and SM22 $\alpha$ ), AVICs were cultured in DMEM with 1% serum. For all assays of phosphorylation events, treatments were given in serum free DMEM. Unless otherwise noted, 1  $\mu$ M 5-HT<sub>2B</sub> antagonists (SB204741 and SB228357, both from Tocris) were added 30 min prior to the addition of 1 ng/ml active TGF- $\beta$ 1 (R&D Systems). SB204741 was chosen due to its high selectivity to 5-HT<sub>2B</sub> ( $pK_i = 7.95$ ) compared to the closely related 5-HT<sub>2A</sub> ( $pK_i < 5.2$ ) and 5-HT<sub>2C</sub> ( $pK_i = 5.82$ ) receptors [18]. SB228357 is a mixed 5-HT<sub>2B/2C</sub> antagonist that is orally active and has been shown to display inverse agonist properties [19] at 5-HT<sub>2C</sub>. Given that 5-HT<sub>2C</sub> receptors have been shown to be minimally expressed in AVICs [11] (supported by PCR data in our lab), we chose to use this as an additional 5-HT<sub>2B</sub> antagonist in the present study. Concentrations of the antagonists were chosen to ensure maximum receptor binding based upon the  $pK_i$  values given by the manufacturer and crude dose response analyses performed in our laboratory to determine efficacy and potency of TGF- $\beta$ 1 inhibition. Small molecule inhibitors of Alk5 (2  $\mu$ M SB431542, Tocris), p38 (10  $\mu$ M SB203580, Tocris), or Smad3 (10  $\mu$ M SIS3, Sigma) were also added 30 min prior to TGF- $\beta$ 1 in appropriate samples.

### AVIC Viability and Proliferation Assay

AVIC viability was assessed using Calcein AM (Invitrogen) and propidium iodide (Invitrogen) stains. Calcein AM is cleaved by esterases within viable cells to exhibit a green fluorescence, and propidium iodide emits red fluorescence only after traversing the compromised plasma membrane of non-viable cells and binding to DNA. Therefore, viable cells were identified by green, but not red, fluorescence, and non-viable cells were identified by red, but not green fluorescence. A positive control was utilized to ensure efficacy of the viability assay by fixing AVICs with 3.7% formaldehyde to render them non-viable. To assess proliferation, AVICs were seeded at the same density and treated with one of the two 5-HT<sub>2B</sub> antagonists. After 24 h, AVICs were harvested and counted. The harvested cell counts were then compared to non-treated controls to determine changes in proliferation.

### Electroporation Transfection Protocol

AVICs were harvested via trypsinization and resuspended at  $2 \times 10^6$  cells/ml in cytomix buffer supplemented with ATP and glutathione. This buffer is designed to mimic cytosolic composition in order to maintain cellular homeostasis during poration. This AVIC suspension was loaded into 4 mm electroporation cuvettes along with 20  $\mu$ g of the plasmid to be delivered. AVICs were then subjected to an exponential decay electroporation protocol using a capacitance of 500  $\mu$ F and a peak voltage of 350 V. Following electroporation, the cuvettes were placed on ice for 10 min to allow the AVICs to recover. After this recovery incubation, AVICs were resuspended in culture media and reseeded onto the appropriate growth surface.

### Quantification of Myofibroblast Activation

AVICs were lysed with Cell Lytic M lysis buffer (Sigma) supplemented with protease inhibitor cocktail (Roche) and centrifuged to remove membrane components. The collected cell lysates were frozen at  $-80^\circ\text{C}$  for storage; each frozen cell lysate was thawed and assayed for total protein content using a standard Bradford Assay.  $\alpha$ SMA was quantified using indirect ELISA after verifying antibody specificity by Western blotting. Briefly, 100

$\mu$ l of 5  $\mu$ g/ml cell lysate solution was adsorbed onto the bottom of 96 well plates by overnight incubation in a carbonate/bicarbonate buffer (pH 9.6). The high pH buffer reduces inter-protein interactions to give an even distribution of proteins within the wells. Non-specific binding sites on the well were blocked using 5% milk in phosphate-buffered saline (PBS) for at least 1.5 h at room temperature. Following this step, 100  $\mu$ l of polyclonal antibody to  $\alpha$ SMA (1:200 in blocking solution) was added to each well and allowed to incubate at room temperature for 1.5 h. After washing the wells 3 times with PBS, each plate was incubated for 1 h with a secondary antibody linked to a peroxidase enzyme. Subsequently, the plates were washed thoroughly with PBS to remove unbound secondary antibodies and each well will receive 100  $\mu$ l of a detection substrate that reacts in the presence of peroxidase to give a product with a characteristic absorbance. The absorbance of each well was detected using a plate reader, and the  $\alpha$ SMA content of each sample was compared to a standard curve created using  $\alpha$ SMA peptide to calculate the concentration of  $\alpha$ SMA in each sample.

SM22 $\alpha$  has also been shown to be an early marker of smooth muscle-like differentiation [20], and has been detected in diseased AV leaflets [2]. Therefore, we utilized a partial promoter to SM22 $\alpha$  that was subcloned into a luciferase reporter plasmid (p-441SM22luc) as a measure of SM22 $\alpha$  promoter activity [21]. This vector was introduced into AVICs via electroporation prior to the addition of GPCR antagonist or TGF- $\beta$ 1 treatments. Following electroporation, AVICs were seeded into 12-well plates and allowed to recover for 24 h. After 24 h of the prescribed treatment, AVICs were lysed using 200  $\mu$ l reporter lysis buffer, and 20  $\mu$ l of this lysate solution was added to a well of a 96-well plate. Luciferase activity was detected by adding 100  $\mu$ l luciferase substrate to each well and recording the luminescent product using a plate reader.

### Calcific Nodule Formation and Detection

To study the effects of 5-HT<sub>2B</sub> antagonism on calcific nodule morphogenesis as in [22], AVICs were cultured in BioFlex® culture plates to 100% confluence on the growth surface. After reaching confluence, AVICs were treated with either 1 ng/ml TGF- $\beta$ 1 alone or in combination with 1  $\mu$ M 5-HT<sub>2B</sub> antagonist for 24 h. After this incubation period, the treatments were replaced with cell culture media and subjected to 15% cyclic strain at 0.75 Hz for 24 h. Following this strain regimen, calcific nodules were identified using Alizarin Red staining to assay for calcium phosphate deposition. AVICs were fixed in 3.7% formalin and 1 ml of Alizarin solution was added to each well for 30 min. The wells were then washed thoroughly with PBS and imaged with conventional microscopy. To ensure that the calcific nodules formed were due to an apoptosis-driven dystrophic process, we utilized an Annexin V/propidium iodide apoptosis assay as described previously [22]. Briefly, AVICs were rinsed with PBS and stained with Annexin V conjugated with Alexa fluor 488 (5% solution in Annexin binding buffer; Invitrogen) for 15 minutes to detect apoptotic cells. Propidium Iodide (0.4% solution in Annexin binding buffer; Invitrogen) was used as a counter-stain for necrotic cells. Apoptosis and necrosis images were taken after 24 h of mechanical strain using a fluorescence microscope (Nikon TE300 Inverted Tissue Culture Microscope).

### Assays for Canonical and Non-canonical TGF- $\beta$ 1 Signaling

AVICs were lysed in RIPA buffer either 15 min or 1 h after AVICs were treated with the prescribed treatment. Lysate solutions were centrifuged to remove lipid components, and total protein concentration was determined using a BCA protein analysis. All proteins were denatured by boiling the samples with  $\beta$ -mercaptoethanol, and gel electrophoresis was used to separate the proteins based upon size. Western blotting was then used to assay for pSmad3, pp38, pSrc, and pCas, and antibodies to the total protein of interest (i.e., both

phosphorylated and unphosphorylated forms) were used to establish proper protein loading. PAI-1 promoter activity was also used to assay for canonical TGF- $\beta$ 1 signaling after 24 h of treatment. To assay for this activity, we utilized a partial PAI-1 promoter (p3TP-lux) subcloned into a luciferase reporter plasmid [23]. This plasmid was transfected into AVICs using the electroporation methods described above, and luciferase activity was assayed according to the methods detailed for SM22 $\alpha$  promoter activity.

### Src Plasmids for AVIC Transfection

To examine the effects of Src activity on AVIC phenotype, AVICs were transfected via electroporation with a vector to express a constitutively active version of Src whereby the autoinhibitory site, tyrosine 527, was mutated to express a phenylalanine residue [24]. Transfection of this mutated Src was verified using Western blotting. For real-time fluorescence imaging of Src trafficking within the cell, a wild-type Src plasmid fused to a mCherry fluorescent reporter was transfected into AVICs. Time-lapse images were collected using a spinning disk Nikon Eclipse TE-2000 confocal microscope equipped with a Photometrics Cascade 512B camera. Both Src plasmids were generous gifts from the laboratory of Irina Kaverina.

### Statistical Analyses

The data are reported as the mean of all replicates, and error is given as standard error of the mean (sample sizes < 30). For each experiment the reported n value indicates independent biological replicates. Statistical significance between treatments was determined by one-way ANOVA, and pairwise differences were identified using post-hoc Holm-Sidak testing.

## Results

### 5-HT<sub>2B</sub> antagonism inhibits AVIC activation and calcific nodule formation

Two structurally dissimilar antagonists to 5-HT<sub>2B</sub>, SB204741 and SB228357, were examined for their ability to inhibit TGF- $\beta$ 1-induced myofibroblast activation in isolated porcine AVICs. Consistent with previous studies [1], AVIC activation was induced by incubation with 1 ng/ml TGF- $\beta$ 1 for 24 h, exhibiting a two-fold increase in both  $\alpha$ SMA protein expression and SM22 $\alpha$  promoter activity (Fig. 1A). Treating AVICs with 1  $\mu$ M of either SB204741 or SB228357 for 30 min prior to and continuing during TGF- $\beta$ 1 incubation abrogates TGF- $\beta$ 1-induced myofibroblast activation of AVICs in the same manner as a direct inhibitor of Alk5. The data indicate that 5-HT<sub>2B</sub> antagonism can prevent AVIC myofibroblast activation, an early event in CAVD, so we were also interested in assessing changes in calcific nodule formation, an endpoint in CAVD. Studies indicate that 83% of excised calcific AV leaflets from human patients are dystrophic [25] and appear to be driven by a TGF- $\beta$ 1-induced apoptotic mechanism [4]. Our lab has recently developed a model system that recapitulates the formation of dystrophic calcific nodules *in vitro* [22]; AVICs treated with TGF- $\beta$ 1 for 24 h prior to the addition of 15% cyclic strain for 24 h form robust calcific nodules that are correlated with  $\alpha$ SMA expression. These results are consistent with previous studies that have shown that  $\alpha$ SMA expression is necessary for nodule formation by AVICs in static culture [26] and that TGF- $\beta$ 1 is required for the formation of nodules in mechanically strained excised aortic valve leaflets [27]. Here, AVICs were treated with either 1 ng/ml TGF- $\beta$ 1 or a combination of TGF- $\beta$ 1 and 5-HT<sub>2B</sub> antagonist for 24 h prior to the addition of strain (Fig. 1B). Calcific nodules were identified using Alizarin Red staining to detect calcium accumulations (Fig. 1C), and as shown previously [22], these nodules form via a dystrophic mechanism as indicated by an outer ring of apoptotic AVICs, as indicated by green fluorescent Annexin V, surrounding a red fluorescent propidium iodide stained necrotic core (Fig. 1D). AVICs treated with 1  $\mu$ M SB228357 or SB204741 form significantly fewer and less mature calcific nodules than the TGF- $\beta$ 1 treated positive

control, and 10  $\mu$ M SB204741 further reduces nodules while SB228357 completely inhibits the formation of any calcific nodules. It should be noted that the antagonist treatments did not affect AVIC viability (Fig. 1E) or proliferation (Fig. 1F).

### 5-HT<sub>2B</sub> antagonism prevents TGF- $\beta$ 1-induced p38 phosphorylation

The data indicate that antagonism of 5-HT<sub>2B</sub> inhibits both myofibroblast activation of AVICs as well as calcific nodule morphogenesis *in vitro*. We were next interested in assessing the effects of 5-HT<sub>2B</sub> antagonism on canonical TGF- $\beta$ 1 Smad signaling. Specifically, Smad3 signaling has been shown to direct a wide variety of TGF- $\beta$ 1-induced cellular responses through direct binding of these transcription factors to gene regulatory elements. Plasminogen activator inhibitor-1 (PAI-1) is one example of a protein that is expressed by Smad3 phosphorylation (pSmad3) and nuclear translocation across many cell types [23]. Thus, we used a plasmid construct with a partial PAI-1 promoter region (p3TP-lux) linked to expression of a luciferase reporter gene to assay for canonical TGF- $\beta$ 1 signaling. Interestingly, 5-HT<sub>2B</sub> antagonism does not inhibit canonical TGF- $\beta$ 1 signaling as indicated by pSmad3 and PAI-1 promoter activity (Fig. 2A–B). Due to the lack of canonical changes, we next assessed possible non-canonical interactions. Many studies have focused on non-canonical signaling pathways to explain the myriad of cellular responses induced by TGF- $\beta$ 1 ligand binding. Particularly, p38 MAPK pathways have been identified as key mediators of cellular processes such as cell migration and mesenchymal transformation [10, 28–29], which are characterized by upregulation of contractile elements similar to those identified in myofibroblast activation. TGF- $\beta$ 1 treated AVICs exhibit a 2.3-fold increase in p38 phosphorylation (pp38), which is completely inhibited by both 5-HT<sub>2B</sub> antagonists (Fig. 2A,C). Additionally, a p38 inhibitor mitigates TGF- $\beta$ 1-induced  $\alpha$ SMA expression and SM22 $\alpha$  promoter activity but does not significantly inhibit canonical PAI-1 promoter activity (Fig. 2D). Similarly, p38 inhibition also prevents TGF- $\beta$ 1-mediated calcific nodule formation, while a specific inhibitor of Smad3 does not reduce the formation of calcific nodules by AVICs (Fig. 2E–F).

### Function and spatial location of Src tyrosine kinase are altered by 5-HT<sub>2B</sub> antagonism

TGF- $\beta$ 1-mediated phosphorylation of p38 has recently been shown to be dependent upon phosphorylation of T $\beta$ RII at tyrosine 284 by Src tyrosine kinase [10]. In addition, 5-HT<sub>2B</sub> has been shown to activate platelet-derived growth factor receptors intracellularly via Src activation [30]. Given that 5-HT<sub>2B</sub> antagonism prevents TGF- $\beta$ 1-mediated p38 phosphorylation, we expected an upstream inhibition of Src phosphorylation, which would prevent its interaction with T $\beta$ RII. Therefore, we assessed the effect of TGF- $\beta$ 1 treatment and 5-HT<sub>2B</sub> antagonism on Src phosphorylation at its active site, tyrosine 418 (pSrc). Treating AVICs with TGF- $\beta$ 1 leads to increased levels of pSrc in a manner that is abrogated by treatment with an Alk5 inhibitor, indicating that pSrc induction is downstream of Alk5 activation by T $\beta$ RII after TGF- $\beta$ 1 ligand binding (Fig. 3A). TGF- $\beta$ 1-induced pSrc peaks at 15 min post-stimulation and returns to near control levels after 1 h. Surprisingly, 5-HT<sub>2B</sub> antagonism does not affect pSrc induction after 15 min of TGF  $\beta$ 1 stimulation (Fig. 3B–C). In fact, 1 h treatment with SB228357 alone leads to a significant increase in pSrc, and the combination of either 5-HT<sub>2B</sub> antagonist with TGF- $\beta$ 1 leads to a sustained activation of Src at 1 h. To assess changes in the downstream function of pSrc, we assayed for phosphorylation within the substrate domain of Crk associated substrate (pCas), a major downstream target of pSrc [31]. Interestingly, 5-HT<sub>2B</sub> antagonism reduces pCas to below basal levels even in cases where pSrc is significantly increased (Fig. 3B, D). This finding is unusual since increased Src phosphorylation typically results in increased pCas.

Previous studies have shown that pCas serves as a negative regulator of canonical TGF- $\beta$ 1 signaling by inhibiting phosphorylation of Smad3 [32]. Therefore, we hypothesized that

since 5-HT<sub>2B</sub> antagonism appears to inhibit pCas, pSmad3 is not inhibited and canonical signaling is subsequently enhanced. This can be seen with increasing doses of 5-HT<sub>2B</sub> antagonist in the presence of TGF- $\beta$ 1, which lead to progressive decreases in  $\alpha$ SMA expression after 24 h, while canonical TGF- $\beta$ 1 signaling, as shown by PAI-1 promoter activity, is increased in response to the non-canonical inhibition (Fig. 3E). To verify this counterintuitive response, we examined wild type mouse embryonic fibroblasts (MEFs) and MEFs with genetically deleted Src family kinases (Src, Yes, Fyn; SYF<sup>-/-</sup>) when exposed to TGF- $\beta$ 1. As expected, SYF<sup>-/-</sup> MEFs exhibit significantly less SM22 $\alpha$  promoter activity and significantly higher PAI-1 promoter activity compared to wild type MEFs (Fig. 3F–G), indicating that Src function is important in non-canonical TGF- $\beta$ 1 signaling and is also involved in the suppression of canonical signaling. In AVICs, 5-HT<sub>2B</sub> antagonism may alter the functionality of Src without directly affecting Src phosphorylation to decrease non-canonical but increase canonical TGF- $\beta$ 1 signaling. To examine this hypothesis, AVICs were transfected to express a constitutively active Src (caSrc), whereby tyrosine 527, the autoinhibitory Src phosphorylation site, is mutated to phenylalanine, thereby preventing phosphorylation at this site and the subsequent conformational change that inhibits Src kinase activity. Expression of caSrc significantly increases SM22 $\alpha$  promoter activity in AVICs after 24 h independent of TGF- $\beta$ 1 ligand in the media and in a manner that is completely inhibited by 5-HT<sub>2B</sub> antagonism (Fig. 3H).

Thus far, the data indicate that 5-HT<sub>2B</sub> antagonism leads to a change in Src functionality, independent of Src phosphorylation. This subsequently prevents association with downstream substrates resulting in decreased Cas and p38 phosphorylation, thereby preventing TGF- $\beta$ 1-induced myofibroblast activation in AVICs. Recent studies suggest that endosomal trafficking and changes in the cellular localization of Src may affect its downstream signaling [33]. Therefore, we used confocal microscopy to assess changes in Src trafficking dynamics before and after 5-HT<sub>2B</sub> antagonism. AVICs were transfected to express fluorescently-labeled wild-type Src (Fig. 4A–F), and images were captured after 1 h of treatment once every 15 s for a total of 15 min. AVICs treated with dimethyl sulfoxide (DMSO) vehicle alone indicate free and rapid movement of the fluorescently labeled Src proteins within the cell (Video S1). A representative section of a DMSO-treated AVIC (Fig. 4B) exhibits altered spatial localization of three labeled Src proteins at 1 min and 1.5 min of imaging. To capture the overall Src kinematics across the entire cell an Eulerian approach was used whereby the change in intensity for each pixel is calculated over time as a representative measure of the movement of Src both within and out of the plane of focus. These values were then used to create a heat map of the image with red indicating a high degree of pixel intensity variation (i.e. Src movement) during the 15 min of imaging and blue indicating little variation over time (Fig. 4C). AVICs treated with 1  $\mu$ M SB228357 for 1 h (Fig. 4D) exhibit little change in spatial localization of fluorescently-labeled Src proteins over the course of 1.5 min (Fig. 4E). Similarly, the Eulerian analysis of the 5-HT<sub>2B</sub> antagonist treated AVIC (Fig. 4F) indicates little fluctuation in pixel intensity over the 15 min imaging interval compared to the DMSO-treated control AVIC. The entire time-lapse sequence shows the clear effect of the antagonist over 15 min (Video S2).

## Discussion

The major impact of this study is three-fold: 1) non-canonical p38, but not canonical Smad3, signaling is required for TGF- $\beta$ 1-mediated myofibroblast activation in AVICs, 2) non-canonical TGF- $\beta$ 1 signaling, and thus myofibroblast activation of AVICs, can be arrested by 5-HT<sub>2B</sub> antagonism, and 3) 5-HT<sub>2B</sub> antagonism physically restricts Src, preventing downstream signaling. The relative contributions of Smad3 and p38 signaling in AVICs were previously unknown. These data indicate that TGF- $\beta$ 1 signaling activates both canonical Smad and non-canonical p38 MAPK pathways, and in AVICs, both appear to

depend on activation of Alk5 after ligand binding (Fig. 5A). Previous studies have demonstrated that activation of Src and non-canonical signaling actually suppresses canonical TGF- $\beta$ 1 signaling [32]. Our results indicate that non-canonical signaling may play a more substantial role in driving myofibroblast activation of AVICs than canonical signaling. Inhibition of p38 was found to completely inhibit TGF- $\beta$ 1-induced upregulation of myofibroblast markers. Additionally, p38 inhibition prevented the formation of calcific nodules by AVICs, whereas inhibition of the canonical Smad3 pathway did not prevent TGF- $\beta$ 1-induced nodule morphogenesis. These results may elucidate new therapeutic targets (in addition to 5-HT<sub>2B</sub> antagonists) that interact with p38 MAPK signaling to inhibit myofibroblast activation of AVICs by TGF- $\beta$ 1.

This study is also the first to indicate a direct interaction between a specific GPCR, 5-HT<sub>2B</sub>, and non-canonical TGF- $\beta$ 1 signaling. Further, we have identified a novel signaling mechanism wherein a physical arrest of Src tyrosine kinase trafficking by 5-HT<sub>2B</sub> antagonism prevents its association with the downstream substrate Cas (Fig. 5B) and likely T $\beta$ R<sub>II</sub>, which prevents pp38 [10]. This action results in an inhibition of non-canonical p38 activation, which is necessary to induce AVIC myofibroblast differentiation, while simultaneously stimulating canonical Smad3 activation and resultant PAI-1 expression, which may be involved in the negative regulation of TGF- $\beta$ 1 activity [34]. PAI-1 inhibits the activation of the protease plasmin from plasminogen. Active plasmin degrades fibrin (a component of the ECM), and has been shown to lead to the activation of latent TGF- $\beta$ 1 [34–35]. The major physiological purpose of TGF- $\beta$ 1-induced myofibroblast differentiation is ECM secretion and remodeling. PAI-1 may then work to inhibit further plasmin activation, thus preventing continued breakdown of the ECM and further activation of TGF- $\beta$ 1 and effectively turning off the ECM repair process. Therefore, enhanced canonical signaling due to 5-HT<sub>2B</sub> antagonism may not be detrimental *in vivo* given the inhibition of non-canonical signaling and resulting decrease in cellular differentiation.

The action of physically arresting Src is most likely due to the stimulation of GPCR endocytosis — a process often involving pSrc [36–37] — due to antagonist binding. These results also provide another potential example of interactions between G proteins and focal adhesion proteins such as Src to alter cytoskeletal function similar to recent reports [38]. We believe that the clinical implications of this study demonstrate the potential for 5-HT<sub>2B</sub> as a druggable target for prevention of CAVD, and may also indicate the potential of targeting other GPCRs that are members of the G $\alpha$ q family in a tissue-specific manner to prevent fibrosis. Interestingly, antagonists to another G $\alpha$ q GPCR localized to cardiopulmonary tissues — namely, angiotensin II type 1 (AT<sub>1</sub>) receptor blockers (ARBs) — have been successfully utilized in a clinical setting to inhibit excessive TGF- $\beta$ 1 signaling observed in Marfan's syndrome [39–40]. Also of note, AT<sub>1</sub> and 5-HT<sub>2B</sub> have been found to display a functional co-dependence in cardiac fibroblasts, whereby antagonism of one of these GPCRs completely inhibits the other GPCR [16]. Therefore, 5-HT<sub>2B</sub> and AT<sub>1</sub> receptors may also share similar functionality in AVICs. Thus far, however, retrospective epidemiological studies have proven inconclusive on the effectiveness of ARB treatment in reducing CAVD outcomes. Early reports indicated that ARBs were ineffective in preventing the progression of CAVD in high-risk elderly patients [41], but recent studies have presented a more optimistic view on the therapeutic impact of ARBs with patients exhibiting lower scores of AV remodeling [42] and decreased overall cardiovascular outcomes due to AV stenosis [43]. The discrepancy may be one of timing, as it may be important to begin therapeutic intervention at the earliest possible time to prevent the development of CAVD. As indicated in this study, 5-HT<sub>2B</sub> antagonism prevents TGF- $\beta$ 1 myofibroblast activation of AVICs, which we believe to be one of the earliest events in the progression of CAVD. Future studies should consider the relative efficacy of 5-HT<sub>2B</sub> antagonism and ARB treatments in preventing TGF- $\beta$ 1 effects in AVICs. The impact of the current study and future studies



with ARBs would be greatly enhanced by *in vivo* validation; however, at this time there is no ideal animal model for CAVD that recapitulates human pathology. Therefore, to establish a more conclusive understanding of the therapeutic potential of Gα<sub>q</sub> antagonists, randomized controlled studies should be conducted to measure CAVD outcomes in patients taking already approved ARBs or 5-HT<sub>2B</sub> antagonists.

## Supplementary Material

Refer to Web version on PubMed Central for supplementary material.

## Acknowledgments

The authors thank Christopher B. Brown for help in developing many of the protocols and for providing the reporter plasmids used in the study. The mCherry-labeled wild-type Src and caSrc plasmids were kindly provided by Irina Kaverina. The authors would also like to acknowledge Steven K. Hanks, Bryan L. Roth, and Luc Maroteaux for comments on the manuscript.

### Sources of Funding

This work was supported by the AHA (0835496N and 09GRNT2010125), NIH (HL094707), and NSF (1055384), all to WDM. JDH was supported by an AHA Pre-doctoral Fellowship (10PRE4290020). VS was supported by the NIMH Psychoactive Drug Screening Program, U19MH82441, and R01MH61887.

## Abbreviations

<b>AVIC</b>	aortic valve interstitial cell
<b>CAVD</b>	calcific aortic valve disease

## References

- Walker GA, et al. Valvular myofibroblast activation by transforming growth factor-beta: implications for pathological extracellular matrix remodeling in heart valve disease. *Circ Res.* 2004; 95(3):253–260. [PubMed: 15217906]
- Bertipaglia B, et al. Cell characterization of porcine aortic valve and decellularized leaflets repopulated with aortic valve interstitial cells: the VESALIO Project (Vitalitate Exornatum Succedaneum Aorticum Labore Ingenioso Obtenibitur). *Ann Thorac Surg.* 2003; 75(4):1274–1282. [PubMed: 12683575]
- Akat K, Borggreffe M, Kaden JJ. Aortic valve calcification: basic science to clinical practice. *Heart.* 2009; 95(8):616–623. [PubMed: 18632833]
- Jian B, et al. Progression of aortic valve stenosis: TGF-beta1 is present in calcified aortic valve cusps and promotes aortic valve interstitial cell calcification via apoptosis. *Ann Thorac Surg.* 2003; 75(2):457–465. discussion 465-6. [PubMed: 12607654]
- Merryman WD, et al. Synergistic effects of cyclic tension and transforming growth factor-beta1 on the aortic valve myofibroblast. *Cardiovasc Pathol.* 2007; 16(5):268–276. [PubMed: 17868877]
- Howe, PH. Transforming growth factor Beta. In: Thomson, AW.; Lotze, MT., editors. *The Cytokine Handbook*. London: Elsevier Science; 2003. p. 1119-1141.
- Olieslagers S, et al. TGF-beta1/ALK5-induced monocyte migration involves PI3K and p38 pathways and is not negatively affected by diabetes mellitus. *Cardiovasc Res.* 2011; 91(3):510–518. [PubMed: 21478266]
- You J, et al. Osteopontin gene regulation by oscillatory fluid flow via intracellular calcium mobilization and activation of mitogen-activated protein kinase in MC3T3-E1 osteoblasts. *J Biol Chem.* 2001; 276(16):13365–13371. [PubMed: 11278573]
- Compton LA, et al. Transforming growth factor-beta induces loss of epithelial character and smooth muscle cell differentiation in epicardial cells. *Dev Dyn.* 2006; 235(1):82–93. [PubMed: 16258965]

10. Galliher AJ, Schiemann WP. Src phosphorylates Tyr284 in TGF-beta type II receptor and regulates TGF-beta stimulation of p38 MAPK during breast cancer cell proliferation and invasion. *Cancer Res.* 2007; 67(8):3752–3758. [PubMed: 17440088]
11. Fitzgerald LW, et al. Possible role of valvular serotonin 5-HT(2B) receptors in the cardiopathy associated with fenfluramine. *Mol Pharmacol.* 2000; 57(1):75–81. [PubMed: 10617681]
12. Rothman RB, et al. Evidence for possible involvement of 5-HT(2B) receptors in the cardiac valvulopathy associated with fenfluramine and other serotonergic medications. *Circulation.* 2000; 102(23):2836–2841. [PubMed: 11104741]
13. Levy RJ. Serotonin transporter mechanisms and cardiac disease. *Circulation.* 2006; 113(1):2–4. [PubMed: 16391164]
14. Jian B, et al. Serotonin mechanisms in heart valve disease I: serotonin-induced up-regulation of transforming growth factor-beta1 via G-protein signal transduction in aortic valve interstitial cells. *Am J Pathol.* 2002; 161(6):2111–2121. [PubMed: 12466127]
15. Fabre A, et al. Modulation of bleomycin-induced lung fibrosis by serotonin receptor antagonists in mice. *Eur Respir J.* 2008; 32(2):426–436. [PubMed: 18321937]
16. Jaffre F, et al. Serotonin and angiotensin receptors in cardiac fibroblasts coregulate adrenergic-dependent cardiac hypertrophy. *Circ Res.* 2009; 104(1):113–123. [PubMed: 19023134]
17. Maish MS, et al. Tricuspid valve biopsy: a potential source of cardiac myofibroblast cells for tissue-engineered cardiac valves. *J Heart Valve Dis.* 2003; 12(2):264–269. [PubMed: 12701801]
18. Forbes IT, et al. N-(1-methyl-5-indolyl)-N'-(3-methyl-5-isothiazolyl)urea: a novel, high-affinity 5-HT2B receptor antagonist. *J Med Chem.* 1995; 38(6):855–857. [PubMed: 7699699]
19. Bromidge SM, et al. Biarylcarbamoylindolines are novel and selective 5-HT(2C) receptor inverse agonists: identification of 5-methyl-1-[[2-[(2-methyl-3-pyridyl)oxy]-5-pyridyl]carbamoyl]-6-trifluoromethylindoline (SB-243213) as a potential antidepressant/anxiolytic agent. *J Med Chem.* 2000; 43(6):1123–1134. [PubMed: 10737744]
20. Qiu P, Feng XH, Li L. Interaction of Smad3 and SRF-associated complex mediates TGF-beta1 signals to regulate SM22 transcription during myofibroblast differentiation. *J Mol Cell Cardiol.* 2003; 35(12):1407–1420. [PubMed: 14654367]
21. Solway J, et al. Structure and expression of a smooth muscle cell-specific gene, SM22 alpha. *J Biol Chem.* 1995; 270(22):13460–13469. [PubMed: 7768949]
22. Fisher CI, Chen J, Merryman WD. Calcific nodule morphogenesis by heart valve interstitial cells is strain dependent. *Biomech Model Mechanobiol.* 2012
23. Wrana JL, et al. TGF beta signals through a heteromeric protein kinase receptor complex. *Cell.* 1992; 71(6):1003–1014. [PubMed: 1333888]
24. Brabek J, et al. CAS promotes invasiveness of Src-transformed cells. *Oncogene.* 2004; 23(44):7406–7415. [PubMed: 15273716]
25. Mohler ER 3rd, et al. Bone formation and inflammation in cardiac valves. *Circulation.* 2001; 103(11):1522–1528. [PubMed: 11257079]
26. Benton JA, et al. Statins block calcific nodule formation of valvular interstitial cells by inhibiting alpha-smooth muscle actin expression. *Arterioscler Thromb Vasc Biol.* 2009; 29(11):1950–1957. [PubMed: 19679827]
27. Balachandran K, et al. Elevated cyclic stretch induces aortic valve calcification in a bone morphogenic protein-dependent manner. *Am J Pathol.* 2010; 177(1):49–57. [PubMed: 20489151]
28. Wendt MK, Schiemann WP. Therapeutic targeting of the focal adhesion complex prevents oncogenic TGF-beta signaling and metastasis. *Breast Cancer Res.* 2009; 11(5):R68. [PubMed: 19740433]
29. Yu L, Hebert MC, Zhang YE. TGF-beta receptor-activated p38 MAP kinase mediates Smad-independent TGF-beta responses. *EMBO J.* 2002; 21(14):3749–3759. [PubMed: 12110587]
30. Nebigil CG, et al. 5-hydroxytryptamine 2B receptor regulates cell-cycle progression: cross-talk with tyrosine kinase pathways. *Proc Natl Acad Sci U S A.* 2000; 97(6):2591–2596. [PubMed: 10688905]
31. Fonseca PM, et al. Regulation and localization of CAS substrate domain tyrosine phosphorylation. *Cell Signal.* 2004; 16(5):621–629. [PubMed: 14751547]

32. Kim W, et al. The integrin-coupled signaling adaptor p130Cas suppresses Smad3 function in transforming growth factor-beta signaling. *Mol Biol Cell*. 2008; 19(5):2135–2146. [PubMed: 18321991]
33. Sandilands E, Frame MC. Endosomal trafficking of Src tyrosine kinase. *Trends Cell Biol*. 2008; 18(7):322–329. [PubMed: 18515107]
34. Pedroja BS, et al. Plasminogen activator inhibitor-1 regulates integrin alphavbeta3 expression and autocrine transforming growth factor beta signaling. *J Biol Chem*. 2009; 284(31):20708–20717. [PubMed: 19487690]
35. Jenkins G. The role of proteases in transforming growth factor-beta activation. *Int J Biochem Cell Biol*. 2008; 40(6–7):1068–1078. [PubMed: 18243766]
36. Magalhaes AC, Dunn H, Ferguson SS. Regulation of G Protein-Coupled Receptor Activity, Trafficking and Localization by GPCR-Interacting Proteins. *Br J Pharmacol*. 2011
37. Mariggio S, et al. Tyrosine phosphorylation of G-protein-coupled-receptor kinase 2 (GRK2) by c-Src modulates its interaction with Galphaq. *Cell Signal*. 2006; 18(11):2004–2012. [PubMed: 16725308]
38. Gong H, et al. G protein subunit Galpha13 binds to integrin alphaIIbeta3 and mediates integrin "outside-in" signaling. *Science*. 2010; 327(5963):340–343. [PubMed: 20075254]
39. Brooke BS, et al. Angiotensin II blockade and aortic-root dilation in Marfan's syndrome. *N Engl J Med*. 2008; 358(26):2787–2795. [PubMed: 18579813]
40. Habashi JP, et al. Losartan, an AT1 antagonist, prevents aortic aneurysm in a mouse model of Marfan syndrome. *Science*. 2006; 312(5770):117–121. [PubMed: 16601194]
41. Olsen MH, et al. Effect of losartan versus atenolol on aortic valve sclerosis (a LIFE substudy). *Am J Cardiol*. 2004; 94(8):1076–1080. [PubMed: 15476632]
42. Cote N, et al. Angiotensin receptor blockers are associated with a lower remodelling score of stenotic aortic valves. *Eur J Clin Invest*. 2011; 41(11):1172–1179. [PubMed: 21988540]
43. Nadir MA, et al. Impact of renin-angiotensin system blockade therapy on outcome in aortic stenosis. *J Am Coll Cardiol*. 2011; 58(6):570–576. [PubMed: 21798417]

### Highlights

- Non-canonical p38 signaling is required for TGF- $\beta$ 1-induced myofibroblast differentiation
- Non-canonical TGF- $\beta$ 1 signaling can be arrested by 5-HT<sub>2B</sub> antagonism
- 5-HT<sub>2B</sub> antagonism physically restricts Src to prevent non-canonical TGF- $\beta$ 1 signaling

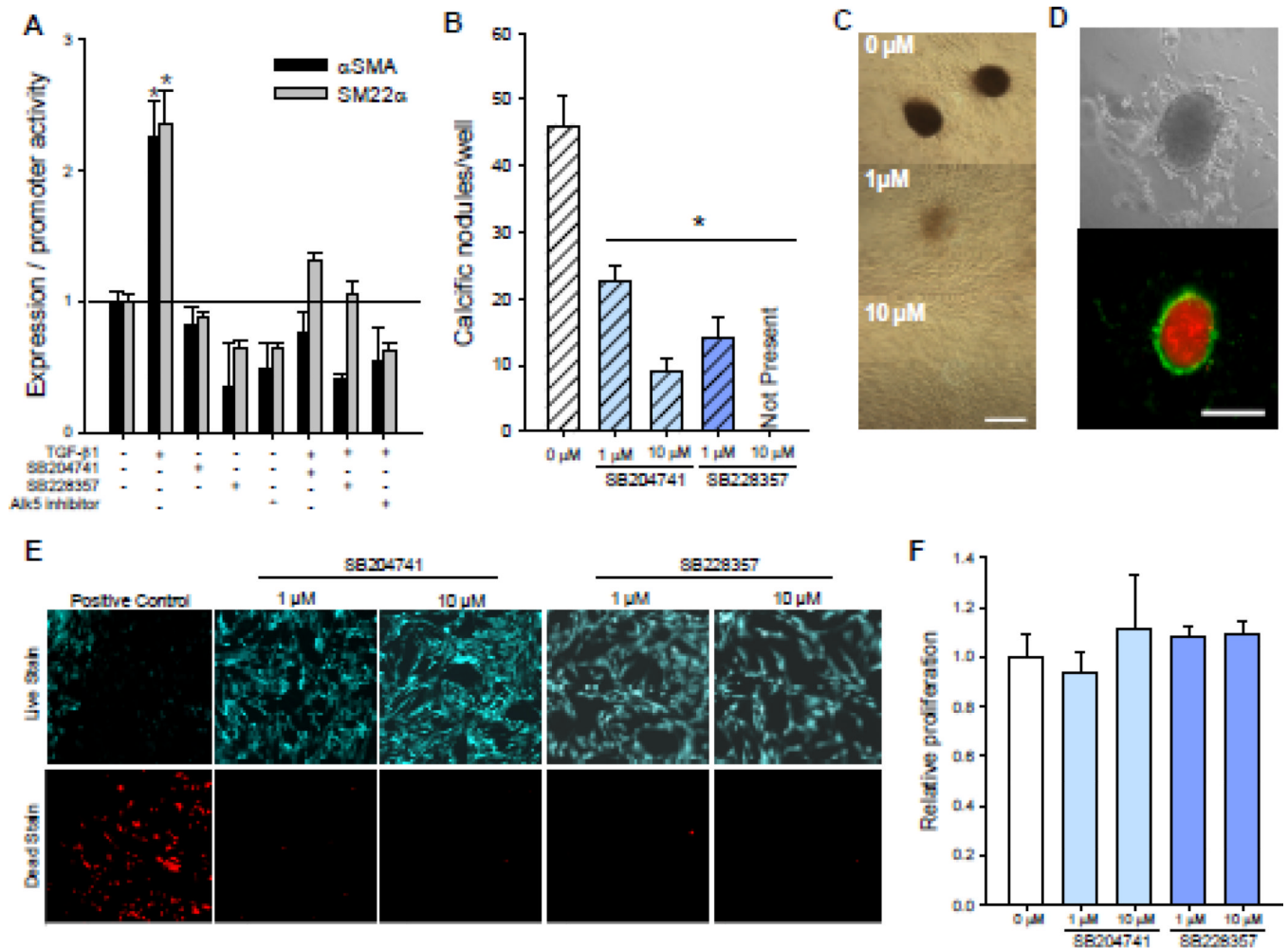


**Fig. 1. 5-HT<sub>2B</sub> antagonism prevents TGF-β1-induced myofibroblast activation and calcific nodule morphogenesis in AVICs**

**A**, Treating AVICs with 1 ng/ml TGF-β1 for 24 h leads to a significant increase in markers for myofibroblast activation, αSMA expression and SM22α promoter activity. Both of these myofibroblast activation markers are reduced to basal levels by pretreating AVICs with either of two 5-HT<sub>2B</sub> antagonists, SB204741 or SB228357, or an inhibitor of Alk5 (n = 3).

**B**, Adding 15% strain to TGF-β1 treated AVICs leads to calcific nodule morphogenesis that is decreased in a dose dependent manner by treatment with SB228357 and SB204741 (p < 0.005, n = 3). **C**, Representative images from samples treated with TGF-β1 and increasing dose of SB228357 demonstrate calcific nodules identified using Alizarin Red. **D**, Calcific nodules were found to be dystrophic with an apoptotic ring (green) of AVICs surrounding a necrotic core (red); bright field (top) and fluorescence (bottom) of a single calcific nodule.

**E**, Neither 5-HT<sub>2B</sub> antagonist affects cell viability. **F**, The 5-HT<sub>2B</sub> antagonists do not affect AVIC proliferation over 24 h. All error bars indicate standard error of the mean. \* indicates significant difference (p < 0.005) versus control. Scale bar = 250 μm.

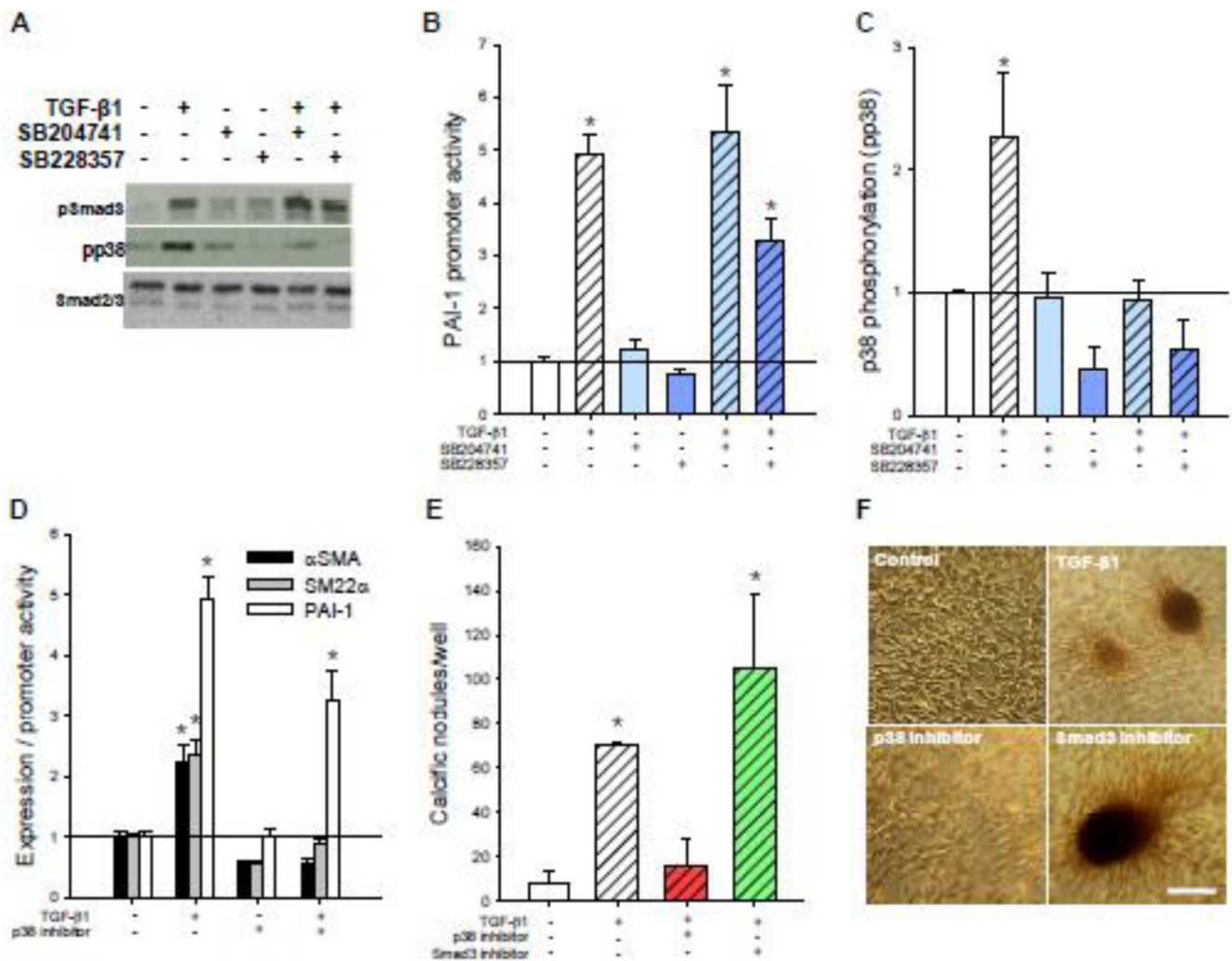


**Fig. 2. 5-HT<sub>2B</sub> antagonism prevents non-canonical p38 MAPK but not canonical Smad3 signaling**

**A**, TGF- $\beta$ 1 treatment leads to increased Smad3 phosphorylation (pSmad3) after 15 min and p38 phosphorylation (pp38) after 1 h. 5-HT<sub>2B</sub> antagonism inhibits TGF- $\beta$ 1-induced pp38 but not pSmad3. **B**, 24 h of TGF- $\beta$ 1 treatment leads to a five-fold increase in canonical PAI-1 promoter activity that is not inhibited by either of the 5-HT<sub>2B</sub> antagonists ( $n = 3$ ). **C**, Average densitometry ( $n = 5$ ) reveals a two-fold increase in pp38 after TGF- $\beta$ 1 treatment that is completely inhibited by 5-HT<sub>2B</sub> antagonism. **D**, p38 inhibitor blocks TGF- $\beta$ 1-induced  $\alpha$ SMA expression and SM22 $\alpha$  promoter activity but not PAI-1 promoter activity. **E**, p38 inhibition blocks TGF- $\beta$ 1-induced calcific nodule morphogenesis but Smad3 inhibitor does not. **F**, Representative images indicate the presence of calcific nodules in AVICs treated with TGF- $\beta$ 1 alone or in combination with Smad3 or p38 inhibitors. All error bars indicate standard error of the mean. \* indicates significant difference ( $p < 0.005$ ) versus control. Scale bar = 250  $\mu$ m.

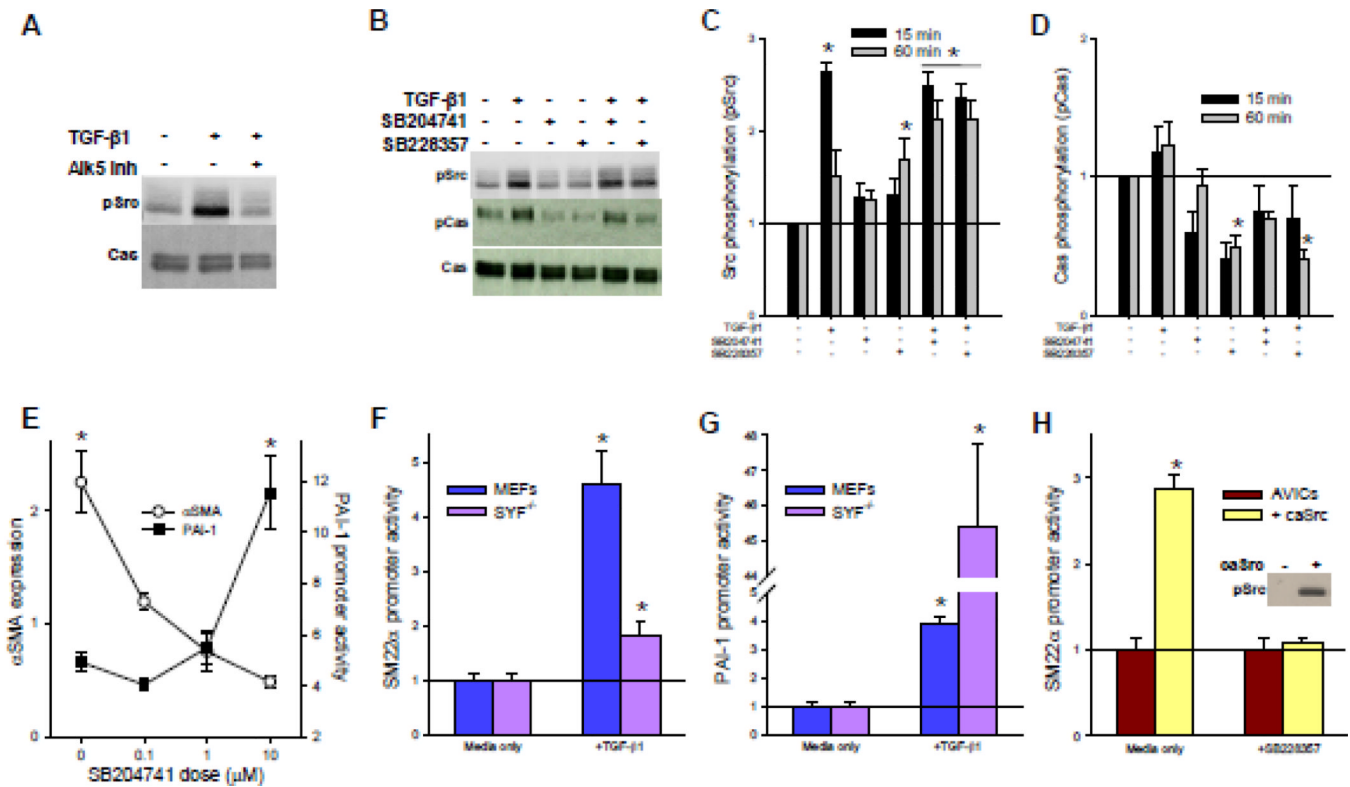


**Fig. 3. 5-HT<sub>2B</sub> antagonism inhibits Src function**

**A**, TGF- $\beta$ 1 induces Src phosphorylation (pSrc) after 15 min of incubation that is inhibited by an Alk5 inhibitor. **B**, Neither 5-HT<sub>2B</sub> antagonist inhibit TGF- $\beta$ 1-induced pSrc; however, pCas is reduced with antagonist treatment in the presence of TGF- $\beta$ 1. **C**, Average densitometry (n = 6) reveal a 2.5-fold increase in pSrc by TGF- $\beta$ 1 at 15 min that return to near basal levels after 1 h. pSrc levels remain elevated in AVICs treated with TGF- $\beta$ 1 and either 5-HT<sub>2B</sub> antagonist after 1 h. **D**, Average densitometry (n = 4) reveals that TGF- $\beta$ 1 treatment leads to a trending increase in Cas phosphorylation (pCas); however, 5-HT<sub>2B</sub> antagonists reduce pCas to sub-basal levels. **E**, Increasing doses of SB204741 lead to decreasing  $\alpha$ SMA but increasing PAI promoter activity in AVICs treated with TGF- $\beta$ 1 (n = 3). **F**, SYF<sup>-/-</sup> MEFs exhibit significantly less SM22 $\alpha$  promoter activity compared to wild-type MEFs following 24 h of TGF- $\beta$ 1 treatment. **G**, SYF<sup>-/-</sup> genetically modified MEFs exhibit a 45-fold increase in PAI-1 promoter activity due to TGF- $\beta$ 1, whereas wild-type MEFs exhibit a four-fold increase in PAI-1 promoter activity. **H**, AVICs transfected to express constitutively active Src (caSrc) exhibit significantly greater SM22 $\alpha$  promoter activity independent of TGF- $\beta$ 1, and SB228357 abrogates this increase. \* indicates significant difference (p < 0.005) versus control.

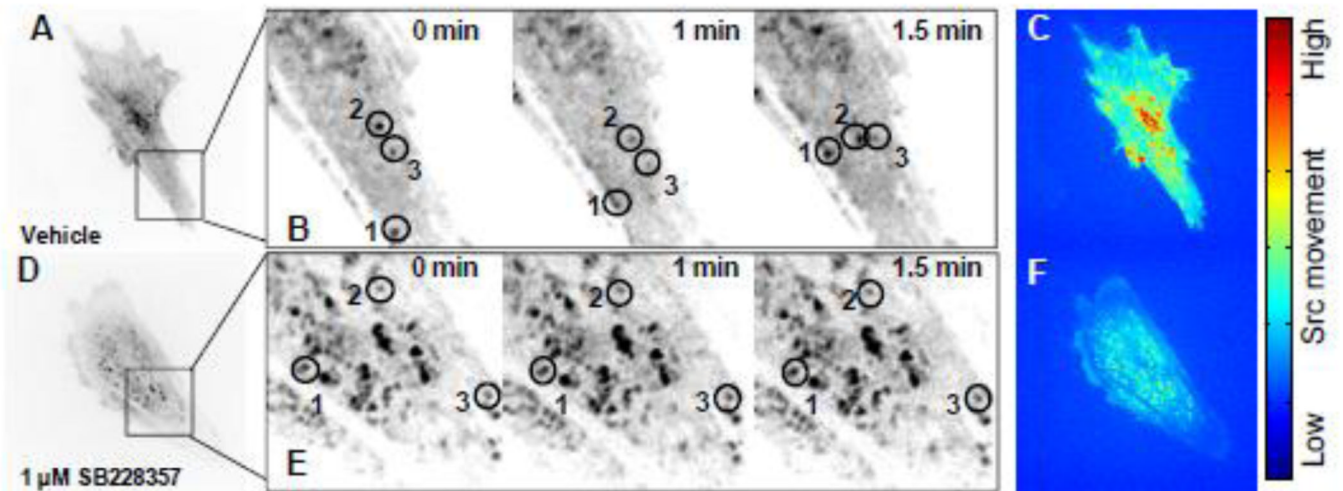


**Fig. 4. 5-HT<sub>2B</sub> antagonism arrests Src motility within AVICs**

**A**, AVICs transfected with mCherry-N1-Src and treated with DMSO vehicle for 1 h were imaged by time-lapse microscopy. Images were taken every 15 s for a total of 15 min. **B**, A subsection of a DMSO vehicle treated AVIC allows for clear identification of Src movement at  $t = 0, 1,$  and  $1.5$  min. **C**, Eulerian based analysis of pixel intensity changes within the image over the course of 15 min represents Src kinematics. Red indicates a high degree of movement, and blue indicates little movement within a pixel. **D, E**, AVICs treated with  $1 \mu\text{M}$  SB228357 for 1 h exhibit little to no Src movement at  $t = 0, 1,$  and  $1.5$  min. **F**, 5-HT<sub>2B</sub> antagonism arrests Src movement over the 15 min imaging time.



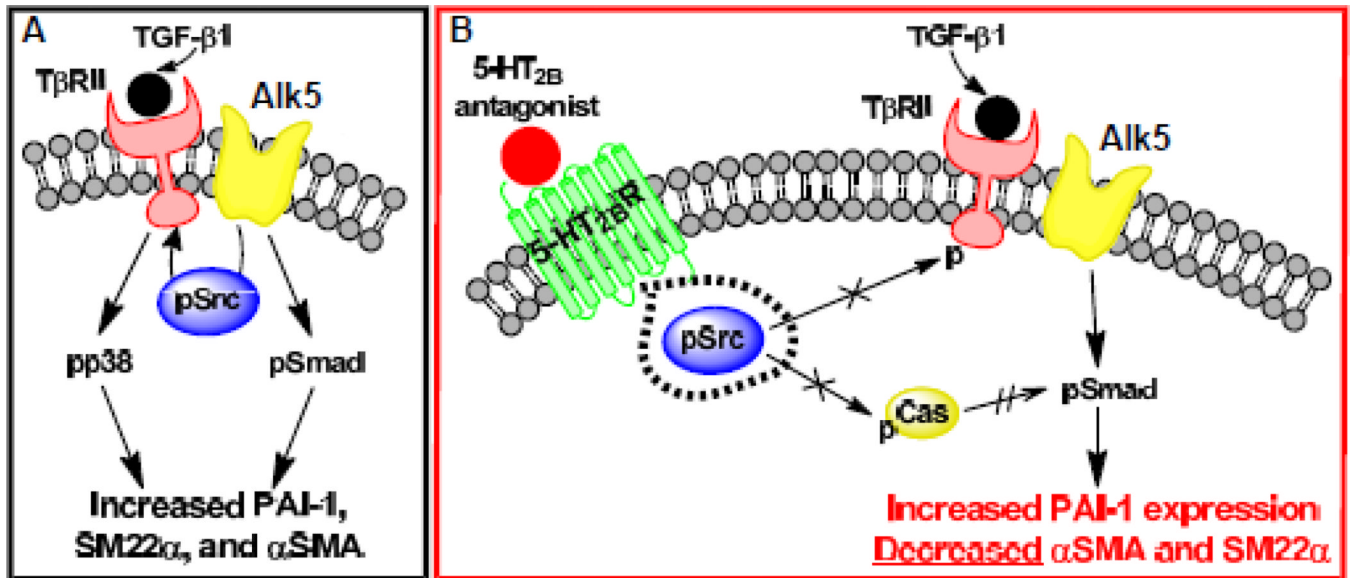


**Fig. 5. Proposed mechanism of 5-HT<sub>2B</sub> antagonist inhibition of TGF- $\beta$ 1 signaling**

**A**, TGF- $\beta$ 1 ligand binding to T $\beta$ RII leads to Alk5-dependent canonical signaling through Smad phosphorylation (pSmad) and non-canonical signaling through Src phosphorylation (pSrc) and subsequent p38 phosphorylation (pp38). **B**, Treatment with a 5-HT<sub>2B</sub> antagonist physically sequesters pSrc preventing non-canonical TGF- $\beta$ 1 signaling by restricting Src's ability to phosphorylate T $\beta$ RII and Cas (indicated with  $\times$  on arrows), but enhancing canonical signaling by suppressing Cas phosphorylation (pCas), which prevents pCas inhibition of pSmad (shown by double hatched arrow).